Thermoelectric coefficients of heavily doped n-type silicon

ISSN 1870-9095

Mulugeta Habte Gebru
Department of Physics, Arba Minch University,Arba Minch, Ethiopia.

E-mail: mulugeta1970@gmail.com

(Received 3 October 2021, accepted 20 November 2021)

Abstract

In this study the thermoelectric effect is investigated in terms of thermoelectric power. The calculations were carried out based on Boltzmann transport equation by taking ionized impurity scattering as a dominant mechanism for heavily doped n-type silicon at 300K with charge concentration varies from $2\mathrm{x}10^{18}/\mathrm{cm}^3 - 20\mathrm{x}10^{20}/\mathrm{cm}^3$. It is known that doping of materials can induce Fermi level shifts and doping can also induce changes of the transport mechanisms. The result of this study shows doping also induces changes in thermoelectric power. The magnitude of the change is different for consideration of parabolic density of states and modified density of states which amounts to 2% on average in favor of the parabolic consideration. There is also on average a 1.44% difference for the calculated values of Peltier coefficient for the two cases in favor of the parabolic consideration.

Keywords: doping, thermoelectric effect, thermoelectric power.

Resumen

En este estudio se investiga el efecto termoeléctrico en términos de potencia termoeléctrica. Los cálculos se realizaron en base a la ecuación de transporte de Boltzmann tomando la dispersión de impurezas ionizadas como un mecanismo dominante para el silicio de tipo n fuertemente dopado a 300K con una concentración de carga que varía de 2x1018/cm3 a 20x1020/cm3. Se sabe que el dopaje de materiales puede inducir cambios en el nivel de Fermi y el dopaje también puede inducir cambios en los mecanismos de transporte. El resultado de este estudio muestra que el dopaje también induce cambios en la energía termoeléctrica. La magnitud del cambio es diferente para la consideración de la densidad parabólica de estados y la densidad modificada de estados que asciende a un 2% en promedio a favor de la consideración parabólica. También hay en promedio una diferencia de 1,44% para los valores calculados del coeficiente de Peltier para los dos casos a favor de la consideración parabólica.

Palabras clave: dopaje, efecto termoeléctrico, energía termoeléctrica.

I. INTRODUCTION

A semiconductor can be considered heavily doped when the impurity band associated with the doped impurity merges with either in the conduction and valence band. There are two aspects with direct influence on the currier transport namely tailing of states into the band gap. It thus seems useful to determine theoretically the location of the Fermi level in heavily doped silicon taking into account the density of states in the tails [1, 2, 3]. According to [1], the density of state for heavily doped silicon is expressed in [4] as

$$\rho(z) = \frac{m_b^{*\frac{3}{2}} 2^{\frac{3}{4}} \delta^{\frac{1}{2}}}{\pi^2 \hbar^3} y(z), \tag{1}$$

whereas,

$$\rho(E) = \frac{8\sqrt{2}\pi m_n^{*\frac{3}{2}}}{h^3} E^{\frac{1}{2}}, \tag{2}$$

represents the parabolic total density of states in the conduction band.

In Eq. (1) for non-parabolic modified density of states, the term y(z) is given by

$$y(z) = \frac{1}{2}\int_{-\infty}^{z} (z-\zeta)^{\frac{1}{2}} exp(-\zeta^2) d\zeta, \tag{3}$$

and

$$z = \frac{E}{\sqrt{2}\delta}. \tag{4}$$

The standard deviation of the Gaussian distribution for the impurity potential energy is

$$\delta = \left(\frac{ne^4 a_s}{8\pi\epsilon_0^2\epsilon_d^2}\right)^{\frac{1}{2}} = \left(\frac{N_d e^4 a_s}{8\pi\epsilon_0^2\epsilon_d^2}\right)^{\frac{1}{2}}. \tag{5}$$

For a screened coulomb potential of impurity atoms with ϵ_d is the dielectric constant of the given semiconductor. The Thomas-Fermi screening length according to [5] is

$$a_s = \left(\frac{\pi^{\frac{\pi}{3}} \epsilon_0 \epsilon_d \hbar^2}{3^{\frac{1}{3}} N_d^{\frac{1}{3}} e^2 m_n^*}\right)^{\frac{1}{2}}. \tag{6}$$

The density of states function given by Equation 1 is very complicated and thus is not useful for making any calculation.

Slotboom [2] has however; suggested the following approximation for *y*(*z*).

$$y(z) \cong z^{\frac{1}{2}}\left[1-\frac{1}{16z^2}\right], \tag{7}$$

for z > 0.601, equally. E > 0.85δ and

$$y(z) \cong \frac{1}{2\pi^{\frac{1}{2}}} exp(-z^2)\{1.225-0.906[1-exp(2z)]\}, \tag{8}$$

for z ≤ 0.601.

Using Eqs. (7) and (8) for *y*(*z*), we obtain the following expression of the electron concentration in the conduction band for modified density of states having band tails

$$n = 2\int f_0\, \rho(E)dE = \frac{m_n^{*\frac{3}{2}} 2^{\frac{5}{4}} \delta^{\frac{3}{2}}}{\pi^2 \hbar^3}\psi_0, \tag{9}$$

where $\psi_0$is obtained by setting λ = 0 into

$$\psi_\lambda = \frac{1}{2\pi^{\frac{1}{2}}}\int_{-\infty}^{0.601} |z|^\lambda exp(-z^2)\left(\frac{0.319+0.906Exp(2z)}{1+Exp\left\{1.494 n_n^{\frac{5}{12}} z-\eta\right\}}\right)dz + \int_{0.601}^{\infty} \frac{z^{\frac{1}{2}}\left[1-\frac{1}{16z^2}\right]}{1+exp\left\{1.494 n_n^{\frac{5}{12}} z-\eta\right\}} dz. \tag{10}$$

It is more convenient to introduce normalized electron concentration n_n given by

$$n_n = \frac{n}{10^{25}/m^3}. \tag{11}$$

In this study the semi-classical and quantum treatments are applied in the calculations of scattering mechanisms under the assumptions of the electron concentrations from 2x1018-2x1020/cm3 and in the temperature range 77 – 300K.

A. Linearized Boltzmann Equation with relation time approximation

All the quantities of interest to us may be expressed immediately in terms of Fermi-Dirac distribution f(r, k.t). The Boltzmann transport equation is therefore

$$\frac{\partial \boldsymbol{f}}{\partial \boldsymbol{t}} + \mathbf{v}.\nabla\mathbf{f} + \mathbf{F}.\nabla_{\mathbf{k}}\mathbf{f} = \left(\frac{\partial \mathbf{f}}{\partial \mathbf{t}}\right)_{\mathbf{c}}. \tag{12}$$

Consider a time dependent but spatially homogenous situation in the absence of applied fields. Thus Eq. (13) becomes

$$\frac{\partial f}{\partial t} = \left(\frac{\partial f}{\partial t}\right)_c, \tag{13}$$

where the term $\left(\frac{\partial \boldsymbol{f}}{\partial \boldsymbol{t}}\right)_{\boldsymbol{c}}$ is expressed in terms of collision operator C as

$$\left(\frac{\partial f}{\partial t}\right)_{\boldsymbol{c}} = C\phi(\boldsymbol{r},\boldsymbol{k}) = \beta\int \boldsymbol{V}(\boldsymbol{k}',\boldsymbol{k})[\phi(\boldsymbol{k}') - \phi(\boldsymbol{k})]\boldsymbol{dk}, \tag{14}$$

for arbitrary function(ϕ) and potential(V). In the relaxation time approximation, we suppose that $\left(\frac{\partial \boldsymbol{f}}{\partial \boldsymbol{t}}\right)_{\boldsymbol{c}}$ has the simplest form which will yield the behavior

$$\left(\frac{\partial f}{\partial t}\right)_c = -\frac{\mathrm{f(K)}}{\tau}. \tag{15}$$

Now for all mechanisms of interest to us, E is not much changed in a single event. For elastic scattering such as ionized impurity scattering this is strictly true, while for acoustic deformation potential scattering (through local band perturbation), it is only approximate. Actually in the cases for which τ is well defined, it is a function of E alone. Thus the relaxation time can be written as

$$\tau = \tau_0 E^\lambda, \tag{16}$$

The value of the superscript λ depends on the scattering mechanism 3/2 for ionized mpurities and -1/2 for acoustic phonons. In the case of optical phonons the electron scattering is not elastic the relaxation time cannot be applied [6].

B. Electron and heat flux densities

In the steady state in a homogeneous system with electric E applied along the x-axis, in the absence of magnetic field, the distribution can be written as

$$f = f_0 + f', \tag{17}$$

which is the solution of

$$-\frac{e}{\hbar}\boldsymbol{E}.\nabla_{\mathbf{k}}\mathrm{f}_0 = \left(\frac{\partial \mathrm{f}'}{\partial \mathrm{t}}\right)_{\mathrm{coll}}, \tag{18}$$

where f_o is the thermal equilibrium distribution and f' is a first order perturbation given by

$$f' = v_x f_x + v_y f_y + v_z f_z. \tag{19}$$

Furthermore,

$$v\left(-\frac{\partial f}{\partial E}\right) = -\frac{1}{\hbar}\frac{\partial f}{\partial k}. \tag{20}$$

And Eq. (19) can be solved to find fx for one-dimensional case using Eqs. 15, 19, and 20 to give

$$f_x = \tau e\left(\frac{\partial f_0}{\partial E}\right)E_x. \tag{21}$$

Since Ex in Eq. (21) is the d.c. electric field is along x-direction, and the x-component of the electric current density is given by

$$J_x = -\frac{2em_n^{*3}}{\hbar^3}\int v_x^2 f_x dv_x dv_y dv_z. \tag{22}$$

Finally after transformation to spherical coordinates (v, θ, φ) for velocity components and making use of Equation 22 for fx , we get

$$J = -\frac{e^2 m_n^{*3} E v_0^5}{6\pi^2 \hbar^3} \int_0^\infty \tau(E) \frac{\partial f_0}{\partial E} \varepsilon^{\frac{3}{2}} d\varepsilon, \tag{23}$$

where we make change of variable from v to $\varepsilon = E/k_BT$.

Thus for the case of parabolic density of states we obtain the following expression for the electrical conductivity

$$\sigma = \frac{2ne^2\tau_0}{m_n^*} \frac{\int_0^\infty \varepsilon^2 f_0 d\varepsilon}{\int_0^\infty \varepsilon^{\frac{1}{2}} f_0 d\varepsilon} = \frac{2ne^2\tau_0}{m_n^*} \frac{F_2}{F_{\frac{1}{2}}}, \tag{24}$$

where $F_{1/2}$ and F_2 can obtained as family of the well known tabulated Fermi-integral by setting p equals to 3 and 4 respectively.

$$\int_0^\infty \frac{\varepsilon^p d\varepsilon}{1+exp(\varepsilon-\eta)}, \tag{25}$$

where $\eta = E_F/k_BT$ is normalized Fermi energy.

We can obtain similar expression for electrical conductivity for the case of non-parabolic modified density of states having band tails in Eq. (1) by inserting into Eq. (24) which gives

$$\sigma = \frac{2e^2 n\tau_0}{3m_n^*} \left(\frac{\sqrt{2}\delta}{k_BT}\right)^{\frac{5}{2}} \frac{\psi_{\frac{5}{2}}}{\psi_0}, \tag{26}$$

where $\psi_{\frac{5}{2}}$ is obtained from Equation 10 by setting λ = 5/2.

To obtain thermal current density, we use from [7]

$$Q_x = \frac{2m_n^{*3}}{h^3} \int \left(\frac{1}{2} m_n^* v^2\right) v_x f d^3 v,$$

$$= = \frac{-4\pi m_n^{*4}}{5\hbar^4} \int_0^\infty v^6 f_x dv, \tag{27}$$

after integrating over spherical coordinates θ and φ.

In the presence of an external d.c. field Ex and a temperature gradient dT/dx along the x-direction, the Boltzmann transport equation is written as

$$v_x \frac{\partial f_0}{\partial x} - \frac{eE_x}{m_n^*} \frac{\partial f_0}{\partial v_x} = v_x \frac{\partial f_0}{\partial x} - \frac{eE_x}{m_n^*} \frac{v_x}{v} \frac{\partial f_0}{\partial v} = -\frac{f-f_0}{\tau} = -\frac{v_x f_x}{\tau} \text{...}(28)$$

One can solve $\frac{\partial f_0}{\partial x}$ in Eq. (28) as

$$\frac{\partial f_0}{\partial x} = \frac{\partial f_0}{\partial T} \frac{\partial T}{\partial x},$$

$$= \left(-\frac{\partial f_0}{\partial E}\right) \left[\frac{E}{T} + k_B T \frac{\partial}{\partial T} \left(\frac{E_F}{k_BT}\right)\right] \left(\frac{dT}{dx}\right). \tag{29}$$

Inserting Eq. (29) into Eq. (28) and solving for f_x, we get

$$f_x = \tau \frac{dT}{dx} \frac{\partial f_0}{\partial E} \left[\frac{E}{T} + k_B T \frac{\partial}{\partial T} \left(\frac{E_F}{k_BT}\right)\right] + eE_x \tau \frac{\partial f_0}{\partial E}. \tag{30}$$

Substituting Eq. (30) into Eq. (23), Jx becomes

$$J_x = -\frac{em_n^{*3}}{3\pi^2 \hbar^3} \int_0^\infty \tau v^4 \frac{\partial f_0}{\partial E} \left[\frac{E}{T} + k_B T \frac{\partial}{\partial T} \left(\frac{E_F}{k_BT}\right)\right] \left(\frac{dT}{dx}\right) dv - \frac{e^4 m_n^{*3} E_x}{3\pi^2 \hbar^3} \int_0^\infty \tau v^4 \frac{\partial f_0}{\partial E} dv. \tag{31}$$

Since a small current flows, Jx = 0 is assumed for measured thermoelectric voltages(V), and the electric field is we obtain the following relationship between Ex and dT/dx.

$$E_x = -\left(\frac{dT}{dx}\right) \frac{\left[\int_0^\infty \tau v^4 \left(-\frac{\partial f_0}{\partial E}\right) \frac{E}{T} dv + \int_0^\infty \tau v^4 \left(-\frac{\partial f_0}{\partial E}\right) k_B T \frac{\partial}{\partial T} \left(\frac{E_F}{k_BT}\right)\right] dv}{e \int_0^\infty \tau v^4 \left(-\frac{\partial f_0}{\partial E}\right) dv\,.} \text{...}(32)$$

If there are no gradients of concentration, then the second term in numerator is cancelled. The Seebeck coefficient(α) referred to as the thermal emf or thermopower [9] is given by

$$\alpha = \frac{dV}{dT} = -\frac{1}{eT} \frac{\int_0^\infty \tau v^4 \left(-\frac{\partial f_0}{\partial \varepsilon}\right) \frac{E}{T} dv}{\int_0^\infty \tau v^4 \left(-\frac{\partial f_0}{\partial E}\right) dv},$$

$$= -\frac{1}{eT} \frac{\int_0^\infty E^4 f_0 dE}{\int_0^\infty E^3 f_0 dE} = -\frac{k_B}{e} \frac{\int_0^\infty \varepsilon^4 f_0 d\varepsilon}{\int_0^\infty \varepsilon^3 f_0 d\varepsilon}$$

$$= -\frac{k_B}{e} \frac{F_4}{F_3}. \tag{33}$$

The Peltier coefficient(Π), which describes how much thermal energy is carried per charge carrier, has primary importance in thermoelectric devices related to Seebeck by Kelvin relation[10],

$$\Pi = -T\alpha = \frac{k_BT}{e} \frac{F_4}{F_3}, \tag{34}$$

for arabolic density of states.

We can obtain expressions for α and Π for the case of modified density of states using the corresponding expressions, i.e., Eq. (34) obtained based on standard model with parabolic density of states (which doesn't incorporate the effect of band tails) by substituting Eq. (1) for modified density of states and by extending the integration limits from -∞ to ∞. This yields the following expressions

$$\alpha = -\frac{\sqrt{2}\delta}{eT} \frac{\psi_{7/2}}{\psi_{5/2}}, \tag{35}$$

and

$$\Pi = \frac{\sqrt{2}\delta}{e} \frac{\psi_{7/2}}{\psi_{5/2}}, \tag{36}$$

where $\psi_{5/2}$ and $\psi_{7/2}$ are obtained from Eq. (10) by setting λ = 5/2 and 7/2 respectively.

II. RESULTS

Thomas-Fermi screening length in Eq.(6) is calculated to be

$$a_s = 7.87X10^{-10} n_n^{-\frac{1}{6}} m, \tag{37}$$

and the value of the Gaussian distribution for impurity potential energy is

$$\delta = 4.375\, X10^{-21} n_n^{\frac{5}{12}} J. \qquad (38)$$

Thus the electron concentration in the conduction band for modified density of states having band tails in Eq. (9) becomes

$$n$$

$$= \frac{m_n^{*\frac{3}{2}} 2^{\frac{5}{4}}}{\pi^2 \hbar^3} \frac{1}{2\pi^{\frac{1}{2}}} \int_{-\infty}^{0.601} \delta^{\frac{3}{2}} exp(-z^2) \left(\frac{0.319 + 0.906 exp(2z)}{1 + exp\left\{1.494 n_n^{\frac{5}{12}} z - \eta\right\}} \right) dz$$

$$+ \int_{0.601}^{\infty} \frac{\delta^{\frac{3}{2}} z^{\frac{1}{2}} \left[1 - \frac{1}{16z^2}\right]}{1 + exp\left\{1.49 n_b^{\frac{5}{12}} z - \eta\right\}} dz,$$

$$= \frac{(1.18)^{\frac{3}{2}} X (9.11)^{\frac{3}{2}} X (10^{-31})^{\frac{3}{2}} X 2^{\frac{5}{4}} X (4.375)^{\frac{3}{2}} X (10^{-21})^{\frac{3}{2}} (0.3)^{\frac{5}{8}}}{\pi^2 X (1.054)^3 X 10^{-102}}$$

$$[\int_{-\infty}^{0.601} (0.28) exp(-z^2) \left(\frac{0.319 + 0.906 exp(2z)}{1 + exp\{1.494 X 0.603 z - \eta\}} \right) dz$$

$$+ \int_{0.601}^{\infty} \frac{z^{\frac{1}{2}} \left[1 - \frac{1}{16z^2}\right]}{1 + exp\{1.49 X 0.603 z - \eta\}} dz \;],$$

$$= 3.2 X 10^{25} \mathrm{X}$$

$$[\int_{-\infty}^{0.601} (0.28) exp(-z^2) \left(\frac{0.319 + 0.906 exp(2z)}{1 + exp\{0.9z - \eta\}} \right) dz$$

$$+ \int_{0.601}^{\infty} \frac{z^{\frac{1}{2}} \left[1 - \frac{1}{16z^2}\right]}{1 + exp\{0.9z - \eta\}} dz \;]. \qquad (39)$$

Thus

$$n_n$$

$$= 3.2[\int_{-\infty}^{0.601} (0.28) exp(-z^2) \left(\frac{0.319 + 0.906 exp(2z)}{1 + exp\{0.9z - \eta\}} \right) dz$$

$$+ \int_{0.601}^{\infty} \frac{z^{\frac{1}{2}} \left[1 - \frac{1}{16z^2}\right]}{1 + exp\{0.9z - \eta\}} dz]. \qquad (40)$$

Similarly for parabolic density of states

$$n_n = 3.2 F_{1/2}(\eta), \qquad (41)$$

and the rest all integrals are evaluated by inserting them directly in the mathematical v.5 installed in the sun ultra 5 work station computer[11]. and using the above values of n_n and η obtained by an iterative method which use employed in the above simplified expressions which relate them for parabolic and modified density of states cases.

The table of values(in the Appendix part of Table I and II), F1/2(-2.6) is evaluated as

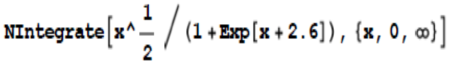

```
NIntegrate[x^1/2 / (1 + Exp[x + 2.6]), {x, 0, ∞}]
```

The result is F1/2(-2.6) = 0.0641614 and the normalized concentration is

$$n_n = 3.2\ F_{1/2}(-2.6) = 3.2{*}0{,}0641614 = 0.2048.$$

Note that iterative method is not one shot process but it takes certain thoughtful steps to get the best value of η which gives to nearest possible value of nn= 0.2 which is η = -2.6. This procedure was followed to evaluate all values in the table including the corresponding values for F3, and F4 for parabolic case.

It is straightforward to use the same procedure for the case of modified density of states. In the same way as the previous case, in the table of values, n_n = 0.2 corresponds to η = -2.9. Mathematica software 5.0 is used to obtain 0.0333945 + 0.13557 = 0.16896 which was taken as the best approximation of nn= 0.2 during the iterating method corresponding to η = -2.9. The same procedure was used for the other pair of values in the table. The values of the other integrals ψ_0 , $\psi_{\frac{5}{2}}$, $\psi_{\frac{7}{2}}$ (in Appendix part of Table II) were evaluated straight forward(even copy and paste of expressions is possible that facilitates th process) by using mathematica v.5.

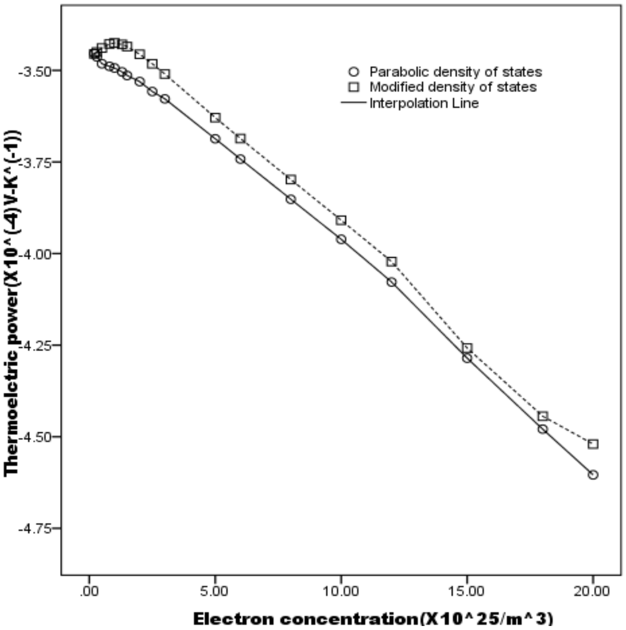

FIGURE 1. shows thermoelectric power as a function of electron concentration with the solid line marked by circles is for parabolic band case and dashed line marked by squares is for modified density of states.

The graph in figure 1 represents the dependence of thermoelectric power, defined as the voltage difference (ΔV) is developed due to temperature difference (ΔT), as a function of electron concentration ranging 0.2 – 20 x $10^{25}/m^3$ for two different cases. On average the calculated values of thermoelectric power differ between considerations of parabolic and modified density of states by 2% in favor of the parabolic density of states consideration.

The graph in Fig. 2 represents the dependence of Peltier coefficient, defined as how much thermal energy is carried per charge carrier, as a function of electron concentration ranging 0.2 - 20 X $10^{25}/m^3$ for two different cases. On average the calculated values of Peltier coefficient differ between considerations of parabolic and modified density of states by 1.44% in favor of parabolic density of states consideration.

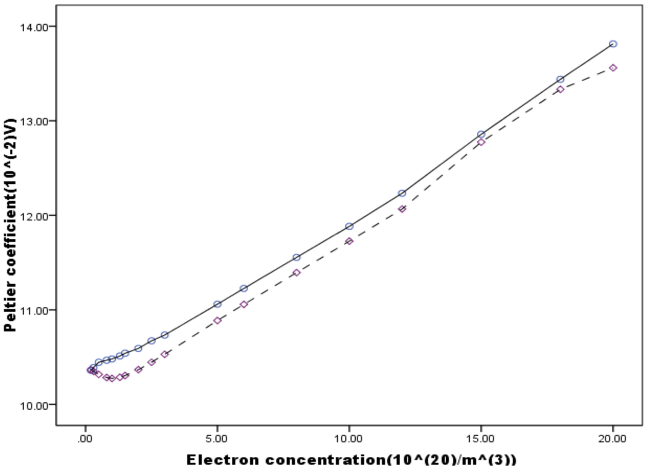

FIGURE 2. shows Peltier coefficient as a function of electron concentration with the solid line marked by circles is for parabolic band case and dashed line marked by squares is for modified density of states.

The experimental result of [12] suggests to use materials in semiconductor group (such as SiC, 6H-SiC, and 4H-SiC), in high temperature, high power applications. It is found that 4H-SiC is more preferable because of its higher electron mobility. The heavily doped silicon can be used instead at high temperature for the reasons indicated in the present study (i) relatively higher electron mobility the reason is that there is considerable shift in Fermi level as carrier concentration gets higher(refer Table A & B in appendix part) that effectively narrows the band gap (ii) thermoelectric power gets higher as the currier concentration gets higher that indicates the possibility to pump the heat out from the device that enables it to function at higher temperature. (iii) Peltier coefficient, on the other hand, indicates recycling of the energy (leakage heat current) that increases the device yield and efficiency. Based on [13] there are also common resistivity losses, for instance, the interaction between the semiconductor and the metallic contact of the solar cell. The use of poor thermoelectric materials may cause the device inefficiency due to energy transfer, recycling or carrier diffusion, for instance, we can replace the metallic contact with good thermoelectric materials as can be suggested from the result of this study.

As an extension to this study it is important to focus on minority-carrier transport in heavily doped silicon. The experimental and theoretical efforts that address such important issues are (i) the incomplete understanding of the minority-carrier physics in heavily doped Si, (ii) the lack of precise measurements for the minority-carrier parameters, (iii) the difficulties encountered with the modeling of transport and recombination in nonhomogeneously doped regions, and (iv) problems with the characterization of real thermoelectric materials [14].

III. CONCLUSION

The thermoelectric effect is investigated in terms of thermoelectric power and Peltier coefficient which have primary importance in device application. There is considerable difference of 2% on average between calculated value of thermoelectric power based on the parabolic density of states and the modified density of states in favor of the former case. The difference between Pelier coefficient values calculated for two cases is 1.44% on average in favor of the parabolic case that is significant as well. The same trend is expected for the electron concentration exceeding $2x10^{26}/m^3$. Laws of modern physics are used in the derivation of modified non-parabolic density of states to make corrections for parabolic density of states consideration as applied for heavily doped silicon, in doing so we can get significant agreement with experimental results.

REFERENCES

[1] Kane, E. O., *Thomas-Fermi approach to impurity semiconductor band structure*, Phys. Rev. **133**, 79-88, (1963).

[2] J. W. Slotboom, J.W., Solid-state Electron 1977, **20**, 279-283(1977).

[3] Hwang, C. J., *Calculation of Fermi energy and band tail parameters in heavily doped and degenerate n-type GaAs*, *J. Appl. Phys.,* **41**, 2268-2674, (1970).

[4] Gebru, M. H., *Electrical and thermal conductivity of heavily doped n-type silicon*, *Eur. Phys. J. Appl. Phys*. **90**, 10102 (2020), available in <https://doi.org/10.1051/epjap/2020190332>

[5] Kittel, C., *Introduction to solid state physics*, (John Wiley & Sons, Inc., New York, 1996).

[6] Cantarero, A. & Àlvarez, F. X. *Springer*, available in <https://www.springerprofessional.de/en/ /2030750>.

[7] W. A. Harrison, W. A., *Solid State Theory*, (McGraw-Hill Book Company, Inc. New York, 1976).

[8] Seiltz, F., *The Modern Theory of Solids*, (McGram-Hill book Company. Inc. New York, 1940).

[9] Rowe, D. M., Thermoelectrics handbook: Macro-to-Nano, (Taylor & Fracis Group, New York, 2006).

[10] Cong, H. W., American journal of modern physics, **4** (2018), Doi: 10.11648/j.ajmp. 20180704.13

[11]Wolfram Research, Inc., Mathematica 5.0. 2008.

[12] Kaźukauskas V., Kalendră, V., and Vaitkus J. V., *Effect of trap levels and defect inhomogeneities on carrier transport in SiC crystals and radiation detectors*, Acta physica polonica a, **17**, 107 (2005).

[13] Gallegos R. D., and Alvardo A. S., *Understanding the stationary and transient state of solar array:Model and simulation,*Lat. Am. J.Phys. Educ. **9**, 1508, 1-9, (2005).

[14] del Alamo J. A. and Swanson R. M., *Modelling of minority-carrier transport in doped silicon emitters,* Solid State Electron **30**, 1127 (1987).

APPENDIX

TABLE I. Calculated values for parabolic density of states.

Serial No̲	n_n	η	$F_{1/2}$	F_3	F_4	$\alpha(x10^{-4}VK^{-1})$	$\Pi(x10^{-2}V)$
1	0.2	-2.6	0.064	0.444	1.778	-3.4539	10.3617
2	0.3	-2.2	0.095	0.66	2.65	-3.4631	10.3893
3	0.5	-1.7	0.15	1.08	4.36	-3.4819	10.4457
4	0.8	-1.2	0.24	1.77	7.16	-3.489	10.467
5	1	-0.9	0.32	2.38	9.64	-3.4935	10.4805
6	1.3	-0.6	0.41	3.19	12.96	-3.5041	10.5123
7	1.5	-0.5	0.445	3.51	14.3	-3.5139	10.5417
8	2	-0.1	0.626	5.17	21.163	-3.5306	10.5918
9	2.5	0.2	0.781	6.87	28.337	-3.5576	10.6728
10	3	0.4	0.94	8.288	34.38	-3.5778	10.7334
11	5	1.2	1.56	17.214	73.58	-3.6867	11.0601
12	6	1.5	1.875	22.41	97.230	-3.7421	11.2263
13	8	2	2.5	34.3	153.18	-3.8518	11.5554
14	10	2.4	3.125	47.5	218.15	-3.9611	11.8833
15	12	2.8	3.75	65.06	307.59	-4.0777	12.2331
16	15	3.4	4.688	101.6	504.83	-4.2856	12.8568
17	18	3.9	5.625	144.13	748.52	-4.4793	13.4379
18	20	4.2	6.25	176.12	940.14	-4.6041	13.8123

TABLE II. Calculated values for modified density of states having band tails.

Serial No̲	n_n	η	ϕ_0	$\phi_{5/2}$	$\phi_{7/2}$	$\alpha(x10^{-4} VK^{-1})$	$\Pi(X\ 10^{-2} V)$
1	0.2	-2.9	0.08	0..9627	5.047	-3.455	10.365
2	0.3	-2.57	0.09	0.6821	3.015	-3.45	10.35
3	0.5	-2.09	0.12	0.472	1.6809	-3.439	10.317
4	0.8	-1.69	0.14	0.3227	0.9416	-3.428	10.284
5	1	-1.5	0.15	0.2681	0.7124	-3.425	10.275
6	1.3	-1.28	0.17	0.2167	0.5167	-3.429	10.287
7	1.5	-1.15	0.18	0.1933	0.4351	-3.435	10.305
8	2	-0.89	0.2	0.1533	0.3079	-3.456	10.368
9	2.5	-0.68	0.21	0.1287	0.2373	-3.482	10.446
10	3	-0.49	0.23	0.1125	0.1938	-3.51	10.53
11	5	0.1	0.28	0.0803	0.1156	-3.629	10.887
12	6	0.34	0.3	0.0726	0.0984	-3.686	11.058
13	8	0.77	0.33	0.0642	0.0795	-3.798	11.394
14	10	1.16	0.36	0.0606	0.0704	-3.909	11.727
15	12	1.52	0.39	0.0592	0.0656	-4.022	12.066
16	15	2.0	0.42	0.058	0.062	-4.258	12.774
17	18	2.46	0.45	0.059	0.061	-4.444	13.332
18	20	2.74	0.47	0.0604	0.0608	-4.520	13.56